DOI: https://doi.org/10.14311/TPFM.2026.004

CFD SIMULATION METHODOLOGY VALIDATED FOR MIXED RECTANGULAR TANK EQUIPPED WITH SINGLE AND MULTIPLE IMPELLERS

V. Bílek [1, 2], O. Gebouský [1, 2], J. Haidl [1]

[1] Czech Academy of Sciences, Institute of Hydrology, Pod Paťankou 30/5, Prague 160 00, Czech Republic

[2] Department of Chemical Engineering, Faculty of Chemical Engineering, University of Chemistry and Technology, Technická 5, Prague 166 28, Czech Republic

Abstract

An experimentally validated methodology for practical fluid dynamics modeling of vessels with atypical geometry, which differs from the standard cylindrical baffled vessel with a centrally mounted impeller, is absent. One reason for this is the lack of experimental data measured on such vessels. We measured experimental data for a rectangular tank equipped with a single impeller and a pair of impellers; either Rushton turbines or pitched-blade turbines (mimicking the geometry of the flocculation tanks at water treatment facilities)—using the particle tracking velocimetry (PTV) technique, as presented in the simultaneously published contribution. Accordingly, this study exploits the measured data to extend the range of operational conditions under which the previously proposed methodology has been validated by systematically comparing experimental measurements with simulation results and providing a critical evaluation of their agreement and limitations. The study identified specific limitations of the proposed simulation methodology when applied to flows characterized by strong impeller–impeller interactions and introduced an extension to the methodology that addresses these deficiencies. The resulting approach is suitable for the analysis and numerical simulation of realistic fluid dynamics in stirred apparatuses exhibiting complex flow structures.

Keywords: stirring, RANS, MRF, sliding mesh, PTV, Rushton turbine, pitched blade turbine.

1 Introduction

Mixing is one of the most commonly used unit operations. The *Standard Tank Configuration* (STC), as defined by Rushton [1] in 1950, is still the best-known and best-studied vessel configuration. The STC is a cylindrical tank equipped with four baffles and a centrally positioned impeller, typically a Rushton turbine. The STC configuration attracts the attention of numerous researchers [2–4] concerned with flow dynamics and its analysis using computational fluid dynamics (CFD). Despite the number of studies, there is no consensus regarding the simulation methodology, even for such a relatively simple, well-mixed system. There are conflicting conclusions regarding the acceptability of impeller motion simplification, the suitability of various turbulence models, and the requirements for mesh density for similar cases. This was a reason for our first study [5] concerning the flow simulation methodology based on the flow in the STC, which led to the definition of the foundation of our methodology. The key requirements were (i) relatively low computational demand, enabling design and optimization on an industrial scale, and (ii) sufficient accuracy in the description of fluid dynamics (high/low mixed regions, main flow loops, dead zones, approximate shear rate distribution).

We started with the STC; despite the fact that our target is to define a methodology that also works for non-standard vessels with atypical configurations. The problem is that a minimum of studies [6, 7] is interested in non-standard vessels; furthermore, they lack validation due to insufficient experimental data. Even the simulations of the STC are typically validated only against a limited number of sets of experimental data, mostly focused on the impeller region; for example, the majority of studies compare their results to the dataset measured by Wu and Patterson in 1989 [8]. There are only a couple of studies concerning the flow characteristics in the entire STC vessel, e.g., Costes and Couderc (1988) [9], Murthy and Joshi (2008) [10], and Płusa et al. (2021) [11], which enabled a more comprehensive validation of our flow simulation methodology.

The next step was to prove the reliability of our methodology for the atypically designed yet industrially relevant stirred vessel. The vessel arrangement in question is a large volume (100-1000 m^3) rectangular tank equipped with multiple radial impellers mounted sideways. That arrangement is commonly found in drinking water and wastewater treatment facilities, which is the target industry our study aims to address. Despite their relatively frequent use, there is a complete lack of experimental data on their characteristics, forcing process designers to rely on unverified CFD simulations and a trial-and-error approach. Due to the lack of experimental data on such a non-standard geometry, we conducted measurements of flow fields in a pilot-scale rectangular tank equipped with one and two asymmetrically placed Rushton turbines and pitched-blade turbines using a modified particle tracking velocimetry (PTV) technique. The experimental technique, data processing, and experimental results are presented partially in [12], and in more detail in the second contribution submitted alongside this one. The aim of this study is to extend the validation scope of the proposed methodology by comparing experimental and simulated data for a more complex geometry, mimicking one of the common flocculation tank arrangements frequently used at water treatment facilities.

2 Mathematical model

Fluid dynamics modeling As this paper is a continuation of our previous studies [5, 12], it draws on the mathematical model framework from Idžakovičová's paper [5]. For the flow simulations, two approaches were tested. Both contain the Reynolds-Averaged Navier-Stokes equations (RANS) with a standard $k-\epsilon$ turbulence model [13] as the model basis. The first uses a steady formulation of RANS, and the second uses an unsteady formulation of RANS (URANS). They differ only in the first temporal term of the following equation, which is zero for the steady case:

$$\frac{\partial \overline{\boldsymbol{U}}}{\partial t} + (\overline{\boldsymbol{U}} \cdot \nabla)\overline{\boldsymbol{U}} = -\frac{\nabla(\overline{p} + \frac{2}{3}\rho k)}{\rho} + \nabla \cdot \left[(\nu + \nu_{\mathrm{t}})(\nabla \overline{\boldsymbol{U}} + (\nabla \overline{\boldsymbol{U}})^T)\right] \quad (1)$$

$$\nabla \cdot \overline{\boldsymbol{U}} = 0 \quad (2)$$

where p is the pressure, ρ is the density, $\boldsymbol{U}$ is the velocity, and k is the turbulent kinetic energy. The bars over the symbols denote the Reynolds-averaged variables. Lastly, ν_{t} is the turbulent viscosity calculated using the standard $k-\epsilon$ model, and ν is the fluid kinematic viscosity. Such an approach ensures relatively low computational demands, and the sufficient accuracy of the flow field results has been experimentally validated in the standard vessel [5] as well as in the studied rectangular vessel with a single Rushton turbine [12].

The two models differ in the method of impeller motion modeling. The first model is built based on the methodology successfully validated in [12], using the multiple reference frame (MRF) approach and the steady RANS equations. The second model is built as transient, using the sliding-mesh (SM) approach and is employed only in cases when the MRF-based simulations do not provide acceptable results. For MRF, equations in the rotating reference frame take the form of

$$\nabla \cdot (\overline{\boldsymbol{U}} \otimes \overline{\boldsymbol{U}}_{\mathrm{R}}) + \boldsymbol{\Omega} \times \overline{\boldsymbol{U}} = -\frac{\nabla(\overline{p} + \frac{2}{3}\rho k)}{\rho} + \nabla \cdot \left[(\nu + \nu_{\mathrm{t}})(\nabla \overline{\boldsymbol{U}} + (\nabla \overline{\boldsymbol{U}})^T)\right] \quad (3)$$

$$\nabla \cdot \overline{\boldsymbol{U}} = 0 \quad (4)$$

where $\boldsymbol{U}$ and $\boldsymbol{U}_{\mathrm{R}}$ are the absolute velocity in the inertial frame and the relative velocity in the rotating frame, respectively. Next, $\boldsymbol{\Omega}$ is the angular velocity of the frame relative to the stationary frame, with $\boldsymbol{U} = \boldsymbol{U}_{\mathrm{R}} + \boldsymbol{\Omega} \times \boldsymbol{r}$ and $\boldsymbol{r}$ being the position vector.

Note that for the Sliding Mesh (SM) approach, the equations are typically solved in the inertial frame (unlike MRF, which is in a rotating reference frame). This means the Coriolis force term ($\boldsymbol{\Omega} \times \overline{\boldsymbol{U}}$) disappears, a time derivative is added, and the convective term is modified to account for the moving grid. The sliding-mesh approach resolves the transient interaction between the rotor and stator by physically rotating the rotor mesh domain relative to the stationary stator mesh. Consequently, the governing equations are solved in a transient manner using the Unsteady RANS (URANS) formulation. To account for the motion of the computational grid, the convective term is modified based on the Arbitrary Lagrangian-Eulerian (ALE) principle. The governing equations take the form:

$$\frac{\partial \overline{U}}{\partial t} + \nabla \cdot (\overline{U} \otimes (\overline{U} - U_g)) = -\frac{\nabla(\overline{p} + \frac{2}{3}\rho k)}{\rho} + \nabla \cdot \left[(\nu + \nu_t)(\nabla \overline{U} + (\nabla \overline{U})^T)\right] \quad (5)$$

$$\nabla \cdot \overline{U} = 0 \quad (6)$$

where $\boldsymbol{U}_\mathrm{g}$ represents the velocity of the mesh. In the stationary stator domain, $\boldsymbol{U}_\mathrm{g} = 0$, whereas in the rotating rotor domain, the mesh velocity is defined as $\boldsymbol{U}_\mathrm{g} = \boldsymbol{\Omega} \times \boldsymbol{r}$. The communication between the stationary and rotating parts of the mesh is handled via a sliding interface that interpolates flow variables across the non-conformal boundary at each time step.

Boundary and initial conditions The water at 20 °C was used as a working fluid ($\nu \approx 10^{-6}\,\mathrm{m^2\,s^{-1}}$). To all stationary physical boundaries (walls and lid), a no-slip boundary condition was prescribed for velocity. For the boundaries of the impellers, the respective impeller velocity was prescribed. The zero-gradient boundary condition for pressure was imposed on all boundaries. To ensure the accurate resolution of the boundary layer across varying mesh densities (y^+), the Enhanced Wall Treatment was applied for turbulence quantities (k, ϵ, ν_t). For the steady simulations, the initial conditions were as follows: fluid at rest, zero for pressure, and ν_t, $k = 10^{-5}\,\mathrm{m^2\,s^{-2}}$, $\epsilon = 10^{-2}\,\mathrm{m^2\,s^{-3}}$. For the URANS formulation, the initial conditions differ only for $k = 0.3\,\mathrm{m^2\,s^{-2}}$ and $\epsilon = 15\,\mathrm{m^2\,s^{-3}}$. The initial period of the URANS simulation lasted 100 s, followed by a period of 30 s, which serves for the calculation of time averages.

Solving methods Calculations were performed using OpenFOAM v2312 [14]. The equations were solved either by the SIMPLE (simpleFoam) algorithm when using MRF or by the PIMPLE (pimpleFoam) algorithm when using the sliding mesh approach. The second-order upwind scheme was used for divergence discretization, and the second-order limited linear schemes were employed for gradient and Laplacian discretization. The implicit Euler scheme was utilized for temporal terms to enhance simulation stability. The time step was chosen to be constant to limit the maximum Courant number below 3, as a compromise between the simulation computational costs and stability. The shift of the edge of the rotating zone is equal to 1.4×10^{-3} m in one iteration. The lengths of the cells' edges on both the inner and outer edges of the boundary of the stationary and rotating zones are approximately 10^{-2} m.

Evaluation metrics The accuracy of the simulation results was evaluated using the experimental data obtained from the particle tracking velocimetry (PTV) technique. The quantities compared were primarily the steady/averaged velocity field and the turbulence kinetic energy. The turbulence kinetic energy was calculated from the measured 2D data, assuming turbulence isotropy:

$$k = \frac{1}{2}\left(\overline{U_x'^2} + \overline{U_y'^2} + \overline{U_z'^2}\right) \approx \frac{3}{4}\left(\overline{U_x'^2} + \overline{U_y'^2}\right) \tag{7}$$

where the prime symbol over U denotes instantaneous velocity fluctuations.

3 Geometry and computational mesh design

Geometry The studied geometry is a rectangular tank with a water volume of 195 L, sketched in Fig. 1.The tank was equipped either with a single 4-bladed pitched-blade turbine in a distance of 410 mm from the side wall, as in the previous study [12], or with two identical impellers, as depicted in Fig. 1. The impellers were either the 6-bladed Rushton turbine (a radial impeller used in previous studies [5, 12]) or the 4-bladed pitched-blade turbine (an axial impeller chosen to expand validated operating conditions), as depicted in Fig. 2 and 3. The presented design and chosen mixing intensities reflect the aim of our research to validate the methodology for flows with highly turbulent as well as poorly mixed zones. Specifically, the mixing intensities correspond to estimated mean velocity gradients of 40 $\mathrm{s^{-1}}$ and 100 $\mathrm{s^{-1}}$, which is the range of intensities recommended when designing flocculation tanks at water treatment facilities. Specifically, the RT rotation speeds were 0.94 $\mathrm{s^{-1}}$ and 1.8 $\mathrm{s^{-1}}$, and the PBT rotation speeds were 1.6 $\mathrm{s^{-1}}$ and 2.84 $\mathrm{s^{-1}}$ for pairs of turbines. For experiments with a single pitched-blade turbine, the respective rotation speeds were 2 $\mathrm{s^{-1}}$ and 3.75 $\mathrm{s^{-1}}$.

Computational mesh The study follows from our previous paper [12], which included a mesh-size independence study of the studied vessel; therefore, this study uses the same cell density structure. There is a finer mesh close to the impeller with a characteristic dimension of 2 mm; the second finer zone around the first one has a characteristic dimension of 4 mm; elsewhere, the cells have a characteristic dimension of 8 mm. At all the wall boundaries, transition layers are added.

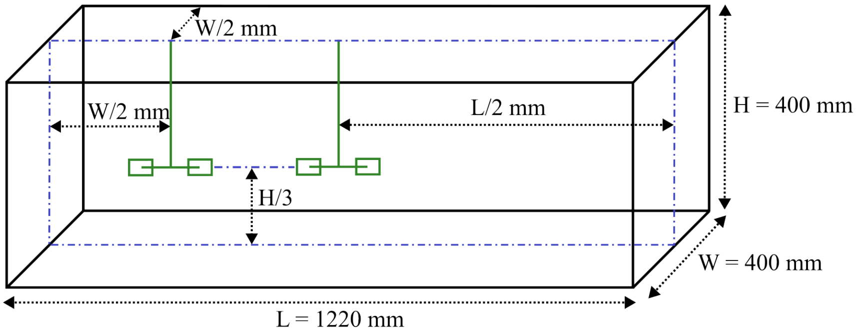

Figure 1: Illustration of the configuration of the asymmetric tank equipped with two impellers – investigated geometry

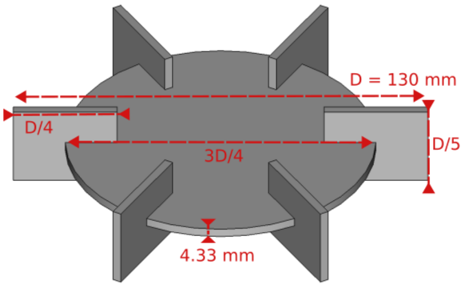

Figure 2: Rushton turbine

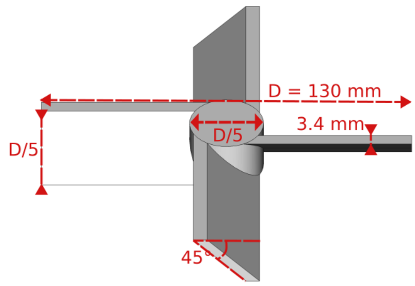

Figure 3: pitched-blade turbine

All the meshes were generated with the snappyHexMesh utility. The generated meshes consist mostly of hexahedral cells, with an arbitrary polyhedral cell in the vicinity of the impellers and in the transition between regions. There are three regions that are stitched together. Two cylinders housing the impellers are designed as a bell-shaped o-grid; the inner cube transitions into a cylinder suitable for the MRF or the sliding mesh. The remaining tank volume mesh is designed as a rectangle with two holes for the cylinders. The resulting mesh for the pitched-blade turbines is shown in Fig. 4. The rotating zones have a diameter of 2.4 D and a height of 1.9 $D/5$, and they have the shape of a perfect cylinder. The characteristic mesh quality metrics are provided in Tab. 1.

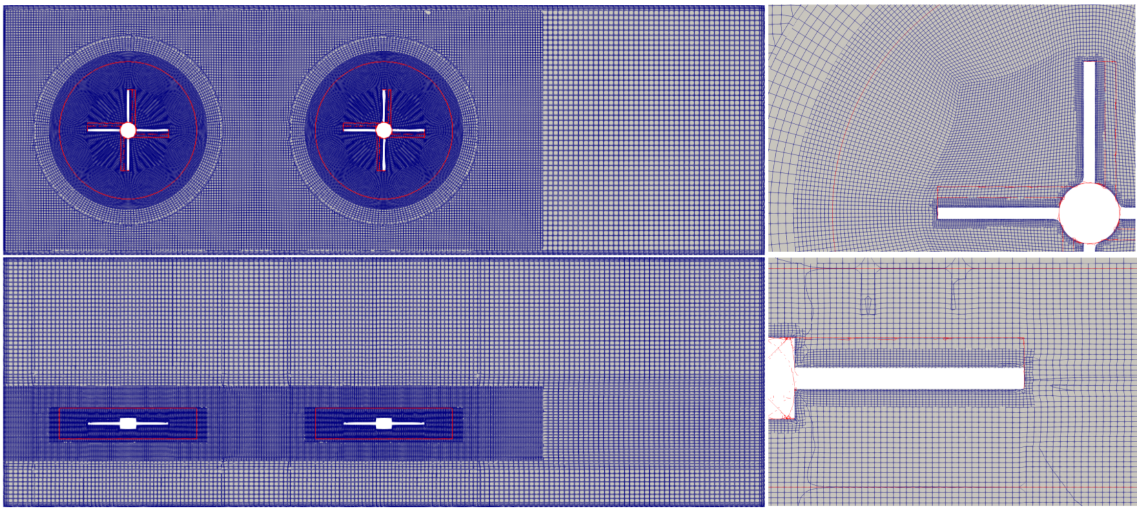

Figure 4: The constructed mesh for two pitched-blade turbines with highlighted rotating zone boundary, top and side views

Table 1: The mesh quality metrics of the mesh in Fig. 4 tank

no. cells	max. non-ortho	avg. non-ortho	max. skewness	max. aspect ratio
4.25 mil	69.7	10.2	2.33	17.0

4 Results and discussion

Single turbine In the previous study [12], the simulation methodology was validated for a single Rushton turbine, and a comparison of the simulation with the experimental data shows that the simulation describes the flow dynamics with sufficient quality. To confirm these findings and extend them to axial turbines, we replaced the Rushton turbine with a pitched-blade turbine. The illustration of the results is depicted in Fig. 5. The conclusions for the pitched-blade turbine are the same as those for the Rushton turbine. The simulation results are in mutual agreement with the experiments and characterize the flow dynamics in the entire vessel with adequate quality relevant for industrial usage. The limitations visible from the comparison, namely the exact distribution or magnitude of the examined quantities, are the price paid for low computing demands.

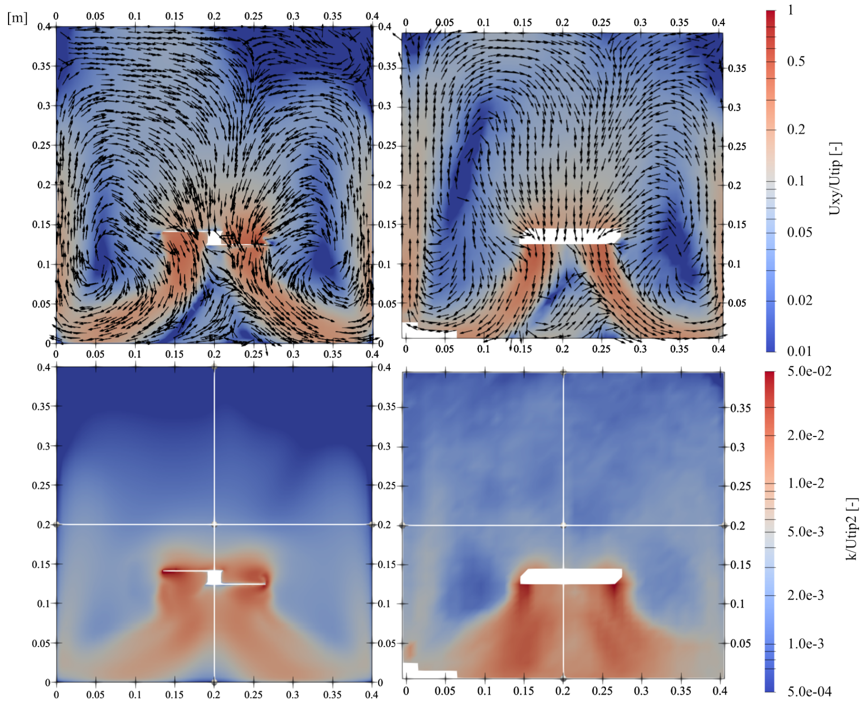

Figure 5: The comparison of velocity and k profiles between the simulation results (left) and the PTV data (right) in side plane 1 cm in front of the shaft, impeller speed = 2 s^{-1}, single pitched-blade turbine

Two Rushton turbines To extend the validated operating conditions, Rushton turbines were the first pair of impellers tested. At first, we used the same methodology: RANS, $k - \epsilon$ turbulence model, and MRF technique. The experimental and numerical results show that there is a strong interaction between the turbines because the radial streams pumped out of the blades meet at high speeds, causing a very turbulent and unstable zone between the impellers. Probably because of this interaction, the RANS-based simulations utilizing the MRF approach for impeller movement are unstable, as illustrated in Fig 6. This instability was independent of the choice of initial conditions, mesh density, and numerical schemes, resulting in unacceptable simulation results. In order to resolve this, two alternative simulation approaches were tested: transient (URANS) simulation with the MRF approach for impeller motion and URANS simulation with the sliding mesh approach, of which only the latter worked acceptably when compared with PTV data.

The time-averaged results for velocity profiles are shown in Fig. 7, where the upper and lower data represent the simulated and measured average velocity fields, respectively. The presented comparison indicates that all the main flow features determined experimentally are present in the simulated data;

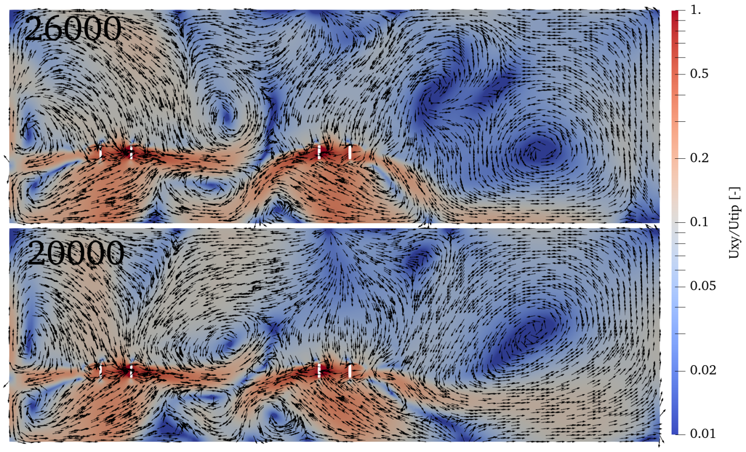

Figure 6: The illustration oscilating behaviour by two convergence states at 20000th and 26000th iteration, RANS, MRF, $k-\epsilon$ turbulence model

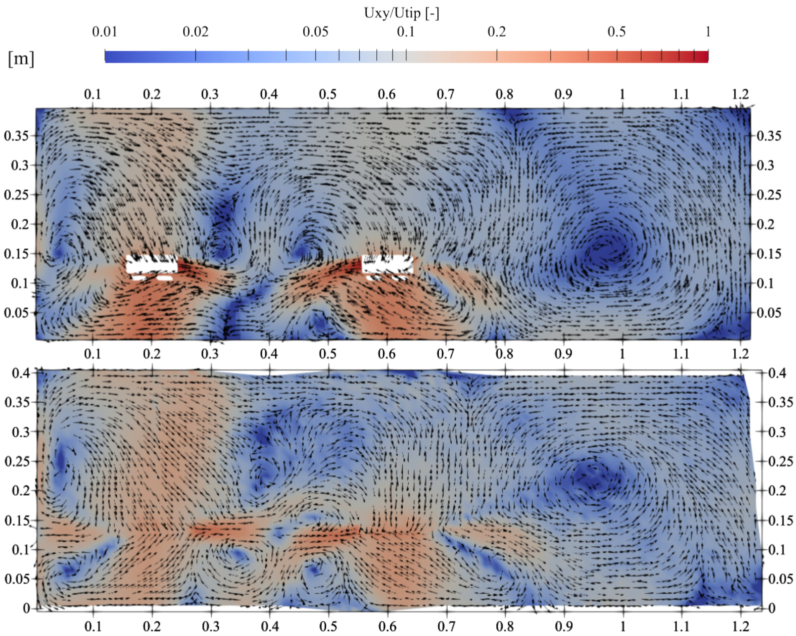

Figure 7: The comparison of velocity profiles between the simulation results (upper) and the PTV data (lower) in plane 5 cm in front of the shaft, impellers speed = 1.8 s^{-1}, two Rushton turbines

however, the exact shape differs and indicates some shortcomings of the standard $k-\epsilon$ turbulence model in modeling complex flow with strong interactions between moving parts. The same conclusions can be drawn for the comparison of the k in Fig. 8. Despite the intrinsic limitations of the model, which are expected when employing RANS-based approaches, these shortcomings should not preclude the application of the methodology to more complex flow configurations. Nevertheless, it remains essential to carefully consider both the model's limitations and its intended range of applicability.

Two pitched-blade turbines To further extend the range of validated simulations, the experiments and simulations performed with double Rushton turbines have been supplemented by arrangements using two pitched-blade turbines—an example of an axial-flow impeller. Unlike the cases of double radial impellers, the RANS-based simulations of axial impellers yielded surprisingly good agreement with the experimental data. The results of the RANS simulation using MRF are shown in Figs. 9 and 10. This difference in

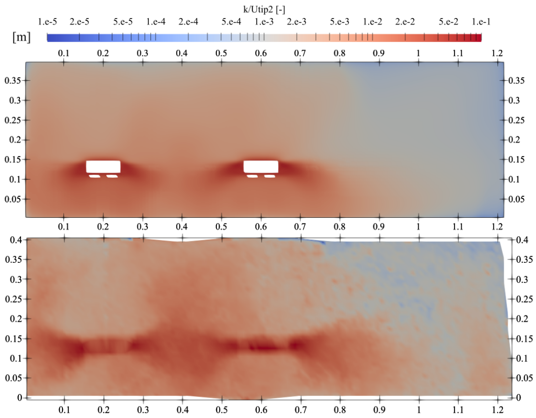

Figure 8: The comparison of k profiles between the simulation results (upper) and the PTV data (lower) in plane 5 cm in front of the shaft, impellers speed = 1.8 s^{-1}, two Rushton turbines

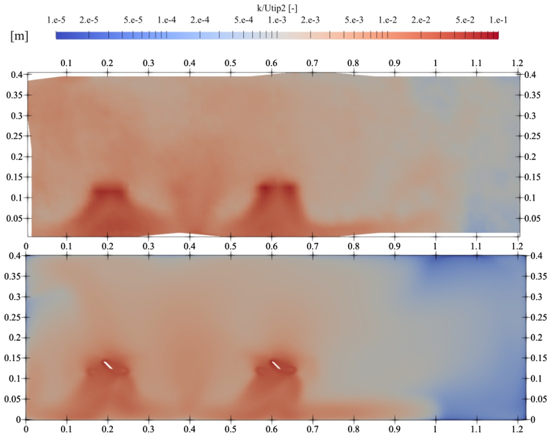

Figure 9: The comparison of k profiles between the PTV data (upper) and the simulation results (lower) in plane 5 cm in front of the shaft, impellers speed = 2.95 s^{-1}, two pitched-blade turbines

simulation convergence and reliability can be attributed to significantly weaker interactions between the impeller jets. Therefore, a stable solution for the simulation of the flow field can be achieved.

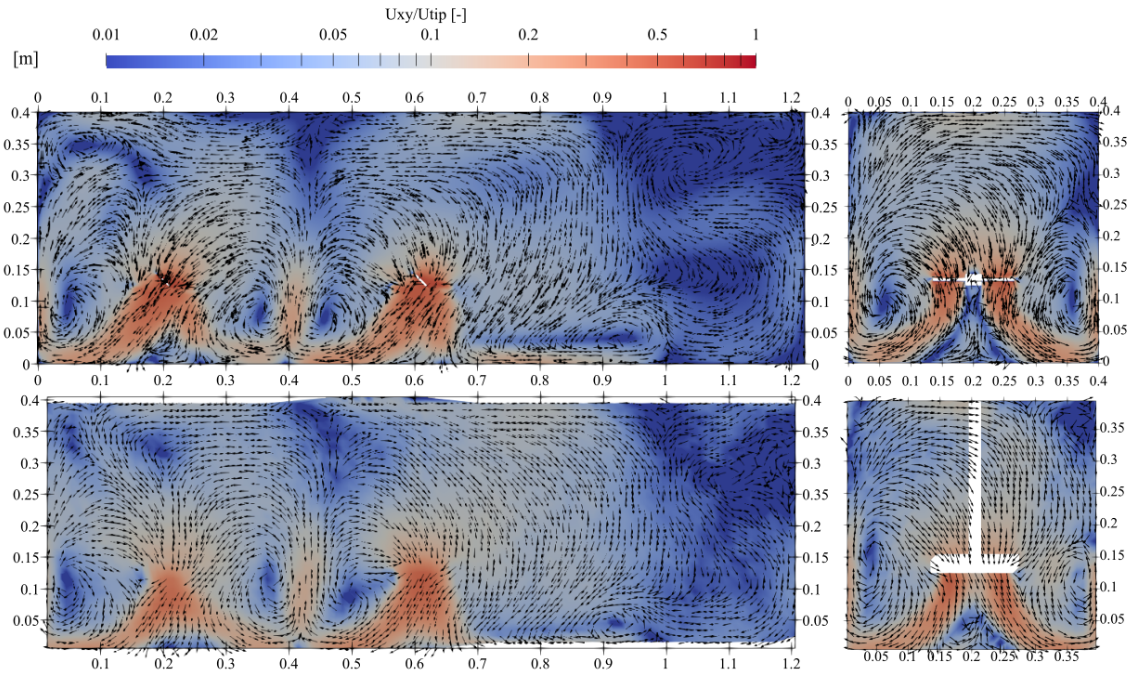

Figure 10: The comparison of velocity profiles between the simulation results (upper) and the PTV data (lower) in plane 5 cm in front of the shaft and side view 1 cm in front of the shaft, impellers speed = 1.6 s^{-1}, two pitched-blade turbines

The results exhibit high mutual agreement in the main flow characteristics—main loops, their positions and shapes, and velocity and k distribution. Overall, the results show the suitability of the presented methodology to describe relatively complex flows; similar to those found, for example, in flocculation tanks at water treatment facilities.

5 Conclusions

The presented paper follows the previous studies of Idžakovičová [5] and Bílek [12] by validating the developed simulation methodology under new operational conditions. For the methodology validation, experimental data obtained by PTV were measured in the configuration of a rectangular tank equipped with either a single pitched-blade turbine or a pair of impellers: either Rushton turbines or pitched-blade turbines. The research revealed the limitations of the methodology for modeling flows with strong interactions between impellers and, thus, the necessity to utilize more computationally demanding techniques to obtain reliable results for such flows, specifically the Unsteady RANS formulation and the sliding mesh approach. Generally, the comparison of the measured and simulated data indicates the methodology's ability to describe relatively complex flows with sufficient quality for industrial tasks. The importance of careful consideration of the model's limitations and intended application remains essential. The practical applicability of the proposed methodology should be confirmed in the following research aimed at modeling industrial flocculators by coupling computational fluid dynamics and population balance modeling.

Acknowledgment

The work on this paper was supported by the institutional support *RVO:67985874*. The research was funded by the *Czech Science Foundation (GAČR)* under *Grant No. 25-17383S*. The participation of VB and OG was financially supported by the *Grant of Specific University Research A1_FCHI_2025_004*. Computational resources were provided by the *e-INFRA CZ project (ID:90254)*, supported by the *Ministry of Education, Youth and Sports of the Czech Republic*.

References

[1] J. H. Rushton, E. W. Costich, and H. J. Everett, "Power characteristics of mixing impellers part 1," *Chemical Engineering Progress*, vol. 46, pp. 395 – 404, 1950.

[2] G. Montante, K. Lee, A. Brucato, and M. Yianneskis, "Numerical simulations of the dependency of flow pattern on impeller clearance in stirred vessels," *Chemical Engineering Science*, vol. 56, no. 12, pp. 3751–3770, 2001.

[3] M. Coroneo, G. Montante, A. Paglianti, and F. Magelli, "CFD prediction of fluid flow and mixing in stirred tanks: Numerical issues about the RANS simulations," *Computers Chemical Engineering*, vol. 35, no. 10, pp. 1959–1968, 2011.

[4] Z. Chára, B. Kysela, J. Konfršt, and I. Fořt, "Study of fluid flow in baffled vessels stirred by a Rushton standard impeller," *Applied Mathematics and Computation*, vol. 272, pp. 614–628, 2016.

[5] K. Idžakovičová, V. Bílek, J. Haidl, M. Isoz, and M. Pivokonský, "Flow simulations approach for flocculation tanks," in *Topical Problems of Fluid Mechanics*, (Prague, Czech Republic), pp. 77 – 84, 2024.

[6] C. Yin, J. He, Y. Xiong, Z. Zhang, X. Luo, Y. Shu, D. Long, and K. Zheng, "Improved suspension quality and liquid level stability in stirred tanks with Rotor-Stator agitator based on CFD simulation," *Particuology*, vol. 82, pp. 64–75, 2023.

[7] S. Gun, S. Chatterjee, and A. Hens, "CFD based analysis of chlorination contact tank design," *Materials Today: Proceedings*, vol. 57, pp. 1813–1818, 2022.

[8] H. Wu and G. Patterson, "Laser-Doppler measurements of turbulent-flow parameters in a stirred mixer," *Chemical Engineering Science*, vol. 44, no. 10, pp. 2207–2221, 1989.

[9] J. Costes and J. Couderc, "Study by laser Doppler anemometry of the turbulent flow induced by a Rushton turbine in a stirred tank: Influence of the size of the units — I. Mean flow and turbulence," *Chemical Engineering Science*, vol. 43, no. 10, pp. 2751–2764, 1988.

[10] B. Murthy and J. Joshi, "Assessment of standard k–ε, RSM and LES turbulence models in a baffled stirred vessel agitated by various impeller designs," *Chemical Engineering Science*, vol. 63, no. 22, pp. 5468–5495, 2008.

[11] T. Płusa, J. Talaga, A. Duda, and P. Duda, "Modeling mixing dynamics in uncovered baffled and unbaffled stirred tanks," *AIChE Journal*, vol. 67, no. 9, p. e17322, 2021.

[12] V. Bílek, O. Gebouský, J. Haidl, and Pivokonský, "CFD simulation methodology for stirred vessels validated by particle tracking velocimetry," in *Topical Problems of Fluid Mechanics*, (Prague, Czech Republic), pp. 15 – 22, 2025.

[13] B. Launder and D. Spalding, "The numerical computation of turbulent flows," *Computer Methods in Applied Mechanics and Engineering*, vol. 3, no. 2, pp. 269–289, 1974.

[14] OpenCFD Ltd., "OpenFOAM - The Open Source CFD Toolbox," 2023.